In vitro and in vivo anti-tumor and anti-inflammatory capabilities of the novel GSK3 and CDK9 inhibitor ABC1183.

Randy S Schrecengost, Cecelia L Green, Yan Zhuang, Staci N Keller, Ryan A Smith, Lynn W Maines, Charles D Smith

Apogee Biotechnology Corporation

1214 Research Blvd, Suite 2014

Hummelstown PA 17036

Running Title. Dual targeting GSK3 and CDK9 with novel ABC1183.

Corresponding Author

Charles D Smith

Apogee Biotechnology Corporation

1214 Research Blvd, Suite 2014

Hummelstown PA 17036

717-531-4758

cdsmith@apogee-biotech.com

Text page count. 27

Table count. 0

Figure count. 6

Reference count. 50

Word Count: Abstract: 165

Introduction: 563

Discussion: 1184

Abbreviations.
CDK – cyclin dependent kinase
CETSA – cellular thermal shift assay
DAI – disease activity index
DAT – Diaminothiazole
DSS – dextran sulfate sodium
GSK – glycogen synthase kinase
GS – glycogen synthase
IBD – inflammatory bowel disease
IP – intraperitoneal
LY – LY2090314
MPO – myeloperoxidase
TNBS – trinitrobenzene sulfonic acid

Selection assignment. Cellular and Molecular

Abstract

Glycogen synthase kinase-3s (GSK3α and GSK3β) are constitutively active protein kinases that target over 100 substrates, incorporate into numerous protein complexes, and regulate vital cellular functions such as proliferation, apoptosis and inflammation. Cyclin-dependent kinase 9 (CDK9) regulates RNA production as a component of positive transcription elongation factor b and promotes expression of oncogenic and inflammatory genes. Simultaneous inhibition of these signaling nodes is a promising approach for drug discovery, although previous compounds exhibit limited selectivity and clinical efficacy. The novel diaminothiazole, ABC1183, is a selective GSK3α/β and CDK9 inhibitor and is growth inhibitory against a broad panel of cancer cell lines. ABC1183 treatment decreases cell survival through G2/M arrest and modulates oncogenic signaling through changes in GSK3, GS and β-catenin phosphorylation and MCL1 expression. Oral administration, which demonstrates no organ or hematological toxicity, suppresses tumor growth and inflammation-driven gastrointestinal disease symptoms, due in part to down regulation of TNFα and IL-6 pro-inflammatory cytokines. Therefore, ABC1183 is strategically poised to effectively mitigate multiple clinically relevant diseases.

Introduction

GSK3α and GSK3β protein kinases regulate diverse cellular functions by incorporating into distinct intracellular complexes and targeting over 100 substrates (Beurel et al. 2015). GSK3 regulates proliferation, in part, through β-catenin (Ha et al. 2004) and c-Myc (Schild et al. 2009), and inflammation through NF-κB-induced cytokine expression, such as TNFα, IL-1β and IL-6 (Beurel et al. 2010). Consequently, excessive GSK3 signaling is implicated in several hyperproliferative and inflammatory diseases including cancer and chronic intestinal inflammation (Hofmann et al. 2010; Walz et al. 2017). Inhibiting GSK3 initially focused on suppressing neuroinflammation in neurologic diseases such as Alzheimer's disease; however, interest in evaluating GSK3 inhibitors as anticancer drugs is growing (Beurel et al. 2015; Duffy et al. 2014; Morales et al. 2014; Vincent et al. 2014).

Post-translational modification of, and by, GSK3 dictates much of the enzymatic activity and downstream signaling output. GSK3α/β Ser21/9 phosphorylation (pSer21/9) by upstream kinases, such as AKT (Cross et al. 1995) and PKA (Fang et al. 2000), is typically viewed as inhibitory since this results in self-substrate priming and occlusion of other primed substrates from GSK3 binding. In general, GSK3 substrates require priming by prior phosphorylation events that enable interaction with the GSK3 binding pocket (Beurel et al. 2015). Therefore, pSer21/9 is one mechanism to regulate activity and substrate selectivity of GSK3. GSK3 activity can also be monitored through downstream signaling. For example, GSK3 mediates serine phosphorylation of glycogen synthase (GS) (Rayasam et al. 2009) and β-catenin (Stamos and Weis 2013) that influences activity or stability, respectively. In the case of β-catenin, only a small subset of total β-catenin is associated with the proteasomal destruction complex and does not affect membrane-bound pools. Overall, measuring multiple post-translational events can give a broad picture of GSK3 activity.

Another enzyme attracting interest as a target for anticancer drugs is cyclin-dependent kinase (CDK) 9 (Krystof et al. 2012; Morales and Giordano 2016). In contrast with most CDKs that regulate the cell cycle, CDK9, in conjunction with cyclin T1, T2a or T2b, forms the catalytic core of the positive transcription elongation factor b (P-TEFb), and thus regulates RNA production. CDK9 is elevated and provides oncogenic transcription profiles in several cancers due, at least in part, to its requirement for transcriptional activation of MYC-targeted genes, such as MCL1 (Gregory et al. 2015; Lam et al. 2001). CDK9 also promotes the expression of inflammatory cytokine genes (Brasier 2008; Brasier et al. 2011) and COX-2 (Keum et al. 2013), and the extravasation of leukocytes into sites of inflammation (Berberich et al. 2011). Mechanistically, CDK9 signals through NF-κB, p38 MAPK, JNK and ERK (Haque et al. 2011; Takada and Aggarwal 2004). Interestingly, pNF-κB is required for CDK9 binding to P-TEFb (Fang et al. 2014; Nowak et al. 2008), and so crosstalk between the GSK3 and CDK9 pathways is critical for inflammatory responses. Therefore, therapies inhibiting both enzymes could potentiate anti-tumor and anti-inflammation pathways to abrogate multiple diseases.

To date, dual GSK3/CDK9 inhibitors have demonstrated non-specific CDK inhibition and shown limited clinical efficacy. Diaminothiazoles (DATs) that inhibit various CDKs or microtubule assembly have been previously described as potent anticancer agents (Thomas et al. 2014; Vasudevan et al. 2015). Here we report the preclinical pharmacological analysis of ABC1183, an orally available novel selective GSK3 and CDK9 inhibitor. The analysis includes kinase inhibition selectivity, *in vitro* cytotoxicity, target modulation, *in vivo* anti-tumor response and *in vivo* anti-inflammatory activity across multiple models.

Material and Methods

Synthesis of ABC1183

4-(4-Amino-2-p-tolylamino-thiazole-5-carbonyl)-benzonitrile (ABC1183). At 0 °C, a mixture of p-Tolyl-isothiocyanate (0.15 g, 1.0 mmol) and cyanamide (0.042 g, 1.0 mmol) in solution of tetrahydrofuran : Methanol (4:1, 5 mL) was treated with Potassium Tert-butoxide (0.124 g, 1.0 mmol) for 30 min. 4-Cyanophenacyl bromide (0.224 g, 1.0 mmol) was added, and the suspension was stirred for 12 h. The solvent was removed, and the semisolid residue was triturated with water to give the crude product, which was filtered and dried in a vacuum oven at 50 °C for 2 h. The dried crude product was recrystallized from EtOAc:Hexane (1:3), which provided 0.170 g (51%) of 4-(4-Amino-2-p-tolylamino-thiazole-5-carbonyl)-benzonitrile (ABC1183) as a yellow solid powder with a melting point of 252-254°C, in methanol. Synthesis and batch-to-batch uniformity was confirmed through HPLC, MS and NMR.

In vitro kinase assay

ABC1183 was screened by ThermoFisher Select Screen Services at a single 10 µM dose against a panel of 414 human kinases using ATP at Km [app]. All kinases were screened in duplicate and data were confirmed to meet stringent quality control standards for reproducibility. Kinases inhibited greater than 60% were further confirmed through dose response IC_{50} assays, carried out by ThermoFisher.

Cell Culture and Treatments

LNCaP human prostate cancer cells were maintained in improved minimum essential media (IMEM) supplemented with 5% FBS and supplemented with 2 mmol/L of L-glutamine. FaDu human squamous cell carcinoma, B-16 F10 murine melanoma, Pan02 murine pancreatic, Mia-Paca2 human pancreatic, BxPC3 human pancreatic and SK-N-MC human neuroblastoma cells

were maintained in DMEM supplemented with 10% FBS. All media was supplemented with 100 U/mL penicillin–streptomycin. ABC1183, LY2090314 and flavopiridol were dissolved in DMSO and treated at indicated concentrations.

SRB assay

To determine IC_{50} values, cells were seeded in 96-well plates and 24 hours later treated with 0 to 100 μM ABC1183 for 72 hours. Cell viability was determined by a standard sulforhodamine B assay as described previously (Schrecengost et al. 2015).

Flow cytometry

Indicated cells were treated and seeded in hormone proficient or depleted conditions, as indicated, and labeled with BrdU (Invitrogen) 2 hours prior to harvest. Cells were fixed in 100% ethanol, stained with FITC-conjugated anti-BrdU antibody (BD Biosciences) and processed using FACS Calibur (BD Biosciences).

Western blot analysis

Cells lysates were produced using buffer containing 25 mM Tris-HCl, 150 mM NaCl, 1% NP-40, 1% sodium deoxycholate, 0.1% SDS (Sigma Aldrich). Total cell lysates were resolved by 10% or 4-12% gradient SDS-PAGE, transferred to PVDF and immunoblotted with the following antibodies: phospho-GSK-3α/β (Ser21/9), GSK-3β, phosph-GS (Ser 641), GS, phospho-β-catenin (Ser33/37, Thr 41), β-catenin, MCL1 (Cell Signaling) and HRP-GAPDH (Genetex).

Cellular Thermal Shift Assay (CETSA)

To determine physical engagement of ABC1183 with target proteins, CETSA was employed as previously described (Jafari et al. 2014; Martinez Molina et al. 2013). Preliminary experiments identified 55˚C as the lowest thermal point for GSK3α/β protein degradation. LNCaP cells were

treated with ABC1183 or DMSO for the indicated times and trypsinized. One half of the cells resuspended in PBS with protease inhibitors, then heated for 3 mins at 55˚C and the other half was not heated to serve as a loading control. If proteins are bound by ABC1183 they will be protected from degradation.

Animal models

All procedures involving mice were performed in accordance with Pennsylvania State University IACUC protocols.

Tumor models: 7 week old male C57BL/6 mice (Jackson Laboratory) were subcutaneously injected in the flank as indicated in 100 µl PBS or PBS/Geltrex (Life Technologies). When tumors reached ~100-150 mm^3 mice were administered 5 mg/kg ABC1183 or Vehicle (50% PEG_{400}, 35% Propanediol, 5% Tween 5% EtOH, 5% Saline) by oral gavage 5 times per week. Body weight was monitored throughout and tumor volume was measured with calipers. Supernatants for the homogenates of each tumor were used to determine the levels of TNFα, IL-6 and IL-1β using Luminex assays performed by the Cytokine Core Laboratory at the University of Maryland, Baltimore. Cytokine values were determined as pg/mL and normalized based on protein concentration to achieve pg/mg of tumor tissue.

TNBS-induced crohn's disease: To model inflammation-induced Crohn's disease, Trinitrobenzene sulfonic acid (TNBS) was utilized for disease onset as previously described (Maines et al. 2010). Briefly, male C57BL/6 mice were anaesthetized and a 0.1 mL solution of 50 µg/g TNBS (Sigma Aldrich) in 50% ethanol/PBS) was slowly administered through a stainless steel catheter carefully inserted into rectum and advanced into the colon until tip was 4 cm proximal to the anus. To ensure retention, mice were inverted for 30 minutes. Colitis was induced by delivery of TNBS on experimental days 0 and 7. Starting on day 6 and proceeding through day 9, animals were treated daily by oral gavage with either Vehicle or 50 mg/kg

ABC1183. On day 10, animals were killed by CO^2 asphyxiation and cervical dislocation, per institutional IACUC requirements, and the colons were removed. The colons were measured, weighed and distal 3 cm was scored for macroscopic inflammation (macro score) as previously described (Fitzpatrick et al. 2000). Supernatants for the homogenates of each colon were used to determine the levels of TNFα, IL-6 and IL-10 using Luminex assays performed by the Cytokine Core Laboratory at the University of Maryland, Baltimore.

DSS-induced ulcerative colitis: To test anti-inflammatory properties of ABC1183, the acute DSS-induced ulcerative colitis model was employed as previously described (Maines et al. 2008). Briefly, male C57BL/6 mice, were divided into groups for Vehicle-only treatment, DSS- (40,000 MW, MP Biomedicals) plus Vehicle treatment, or DSS plus ABC1183 (50 mg/kg) treatments. DSS was administered as 2% solution continuously in drinking water and Vehicle/ABC1183 was administered once daily by oral gavage in a volume of 0.1 mL per dose. The Disease Activity Index, which monitors weight loss, stool consistency and blood in the stool as a measure of disease severity, was scored for each animal on Days 4-6. Mucosal myeloperoxidase (MPO) activity was determined by assaying the middle one-third of colon for MPO by quantifying the metabolism of tetramethylbenzidine as described by Fitzpatrick et al. (Fitzpatrick et al. 2000), as a measure of granulocyte and monocytes infiltration into the colon.

Statistics

All results were analyzed using the 2-tailed Student's *t* test (adjusted for variance) or Mann-Whitney test. For all analyses, $P < 0.05$ was deemed significant.

RESULTS

Specific inhibition of GSK3 and CDK9 activity

A novel diaminothiazole, ABC1183, was designed as described (Fig. 1A). To determine if ABC1183 functions as a selective kinase inhibitor, a panel of 414 human kinases was screened at a single 10 μM dose, as described in material and methods. ABC1183 modulated enzyme activities from -17 to 85 percent, however, only 4 targets, CDK9 (inactive), GSK3α, GSK3β, and CDK9/cyclinT1 were inhibited greater than 60% (Fig. 1B). In fact, despite similarities between GSK3 and CDK ATP binding pockets, CDK2 was the next most inhibited CDK at 44% inhibition. IC_{50} values for ABC1183 against GSK and CDK9 targets were determined to be 657 nM for GSK3β, 327 nM for GSK3α and 321 nM for CDK9/cyclin T1 (Fig 1C). Additionally, ABC1183 was identified as an ATP-competitive inhibitor for both GSK3 isoforms but a non-competitive ATP inhibitor for CDK9/cyclinT1 (Supplementary Fig. S1).
To determine if ABC1183 physically engages with GSK3 in a whole cell setting, cellular thermal shift assays (CETSA) were utilized. Incubation of cell lysates at 55˚C resulted in protein degradation when unbound by ABC1183. However, within 15 minutes of incubation, ABC1183 was able to physically associate with GSK3α and GSK3β, which is sufficient to protect from degradation (Supplementary Fig. S2). Based on these data, we hypothesized that ABC1183 selectively inhibits GSK3α, GSK3β and CDK9.

ABC1183 inhibits cell growth and abrogates signaling

To determine if inhibition of GSK3 and CDK9 activity negatively influences cell proliferation, a panel of murine and human cancer cell lines were treated with increasing concentrations of ABC1183, then analyzed for cytotoxicity. IC_{50} cytotoxicity values, as determined by SRB assay, ranged from 63 nM to 2.6 μM and were similar to *in vitro* kinase inhibition values for GSK3 and CDK9 (Fig. 2A). GSK3 inhibitors have been reported to arrest cell cycle progression while CDK9 inhibitors promote cell apoptosis (Sonawane et al. 2016;

Walz et al. 2017). Analysis of cell cycle phases following treatment demonstrated that, relative to control, ABC1183-treated cells had a significantly decreased number of cells in replicating G1 and S phases, and contained an increased number of cells in G2/M and sub-G1 cycle phases (Fig. 2B). This suggests that ABC1183 is disrupting cellular proliferation by blocking cell cycle progression and promoting cell death.

GSK3α/β activity can be monitored through pSer21/9 levels, downstream GS pSer641, and β-catenin pSer33/37/Thr41. Similarly, MCL1 and RNA Polymerase 2 (Pol2) are major downstream targets of CDK9 activity. To determine if ABC1183 can modulate GSK3 and CDK9 activity within a whole cell environment, multiple cell lines were treated for 2 to 24 hours with ABC1183, or known GSK3 inhibitor, LY2090314 (LY), and cellular signaling was queried. As shown in Figure 3A-C, ABC1183 treatment decreased GSK3α/β pSer21/9 in a time-dependent fashion, although GSK3β was more dramatically decreased compared to GSK3α. Cell-specific differences were also observed, including transiently decreased GSK3β phosphorylation in LNCaP cells (Fig. 3A, lane 2) and a rapid and persistent downregulation of GSK3β phosphorylation in FaDu cells (Fig. 3C, lanes 1 to 4). Consistent with GSK3 inactivation, GS phosphorylation was also decreased in a cell type specific fashion. For example, in LNCaP and FaDu cells, ABC1183 most significantly decreased pSer641 GS 24 hours after treatment (Fig. 3A and C) and to a similar extent as 24 hour LY treatment. Pan02 cells, by comparison, exhibited a less robust inhibition of GS phosphorylation, however, LY treatment was similarly ineffective (Fig. 3B). β-catenin pSer33/37/Thr41, which targets the protein for proteasomal degradation (Stamos and Weis 2013), was increased between 6 and 24 hours following ABC1183 treatment in all cell lines (Fig. 3 and Supplementary Fig. S3). Based on these data, ABC1183 modulates GSK3 activity, which negatively regulates multiple downstream signaling events.

To address inhibition of CDK9, downstream targets were evaluated at protein and mRNA levels. MCL1 total protein levels were measured following ABC1183 treatment and

determined to be decreased most discernibly in LNCaP and Pan02 cells after 24 hours (Fig. 3A and B). There was also a robust decrease in Pol2 activity, measured by pSer5 Pol2, following ABC1183, which was observable to similar levels in cells treated with CDK9 inhibitor, flavopiridol (Supplementary Fig. S4A). Furthermore, the CDK9-regulated gene, *Hexim1,* was detected to be significantly decreased at the mRNA level following 24 hours of ABC1183 treatment (Supplementary Fig. S4B). Overall, these *in vitro* and cell based experiments demonstrate that ABC1183 specifically targets GSK3α/β and CDK9, inhibiting cell proliferation and cell cycle progression and modulating intracellular signaling.

Anti-tumor effects of ABC1183

To extend the anti-proliferative findings of ABC1183 treatment, several allogenic tumor models were employed to understand *in vivo* therapeutic response. First, murine melanoma B16 tumors were propagated in C57BL/6 mice. Following initial tumor growth, mice were treated with oral ABC1183 or Vehicle. As depicted in Figure 4A, tumor growth was decreased more than 70% within 8 days by ABC1183 treatment, relative to vehicle, which was maintained until termination of study. Based on body weight, gross toxicities were not observed (Fig. 4A, right). Next, murine pancreatic Pan02 allograft tumors were propagated and, relative to B16 tumors, exhibited a less aggressive growth kinetics that allowed for extended treatment of tumors. Oral treatment significantly suppressed tumor growth, which was visible by day five and persisted throughout the 22-day treatment course (Fig. 4B). Again, based on body weight, no toxicities were observed. Finally, prostate TRAMP-C2 tumors were treated with oral ABC1183 or Vehicle over the course of 21 days. Throughout the experiment, ABC1183 treatment diminished tumor size, compared to vehicle, and no toxicities were observed (Fig. 4C).

Monitoring pharmaceutical on-target action is critical for understanding response rates in clinical trials. Therefore, to determine if ABC1183 impinges on intratumoral GSK3 signaling, representing a clinically relevant biomarker candidate, previously untreated tumor-bearing mice

were treated with oral ABC1183 (5 mg/kg) or intraperitoneal (IP) ABC1183 (25 mg/kg), for 2 and 12 hours to analyze GSK3α/β phosphorylation and downstream GS phosphorylation. GSK3α/β pSer21/9 was decreased in all treatment groups, compared to Vehicle, with no remarkable changes to total GSK3β expression (Fig. 4D, compares lanes 1 to 3 with 4 to 15). Interestingly, low dose oral treatment was as effective as high dose IP, demonstrating robust oral bioavailability. GS pSer641 levels were also appreciably diminished by all ABC1183 treatment conditions, compared to Vehicle, without altering total GS expression.

Since GSK3 and CDK9 can activate inflammatory signaling pathways, it was also of interest to determine whether inflammatory cytokines within tumor samples were altered in response to ABC1183 administration. Pan02 tumor-bearing mice were treated with vehicle or 25 mg/kg ABC1183 and TNF-α, IL-6 and IL-1β cytokines were quantified from harvested tissue. Consistent with ABC1183 inhibiting GSK3 and CDK9, 12 hours following compound administration intratumoral TNF-α was reduced 65%, IL-6 was decreased 30% and IL-1β was diminished by 45%, relative to control (Supplementary S5). In sum, these tumor models demonstrate that ABC1183 inhibits tumor growth *in vivo*, in part by impinging on GSK3 signaling and reducing inflammatory cytokines. GSK3 and GS phosphorylation levels can also be utilized as pharmacodynamic biomarkers to assess target engagement in tumor samples.

Historically, some GSK3 inhibitors manifested deleterious side effects that halted clinical development (Eldar-Finkelman and Martinez 2011). To begin to identify potential ABC1183 side effects, 100 mg/kg and 200 mg/kg (20 to 40-fold above anti-tumor efficacy) were administered orally for 7 days followed by gross organ analysis and serum chemistry profiles. Heart, liver, kidney and overall body weights, compared to Vehicle, did not differ appreciably (Fig. 5A). Blood chemistry analysis revealed normal levels of red blood cells, white blood cells and platelets. Furthermore, ALT, creatinine and glucose were also measured and normal, with the exception of elevated ALT at the highest 200 mg/kg dose (Fig. 5A). These high-dose, short term exposure

studies, in concordance with the *in vivo* tumor studies, provide evidence that ABC1183 is a safe and efficacious treatment option.

ABC1183 reverses inflammation-induced pathologic IBD

GSK3 isoforms influence disparate disease progression, in part, through pro-inflammatory signaling. Inflammatory bowel disease (IBD) is the clinical manifestation of chronic colonic inflammation, with often debilitating symptoms. To address the ability of ABC1183 to abrogate progression of IBD, disease symptoms were induced by multiple models. First, trinitrobenzene sulfonic acid (TNBS)-induced colitis was modeled. Relative to vehicle alone, rectal TNBS administration on day 0 and 7 resulted in significant incidence of disease within the colon, as determined by macroscopic inspection (Fig. 5B, hatched bars). However, addition of oral ABC1183 on day 6-10 significantly decreased macroscopic symptoms of inflammation, such that these colons were indistinguishable from vehicle. Analysis of cytokines within the colons revealed that TNBS treatment increased the pro-inflammatory cytokines TNF-α and IL-6 (Fig. 5C). Consistent with reduced evidence of inflammation seen through macroscopic inspection, TNFα and IL-6 levels in colons were reduced 60% and 85%, respectively, in ABC1183-treated animals. Therefore, TNBS-induced colitis represents a scenario where ABC1183 treatment is sufficient to reverse or diminish the negative physiologic effects of inflammation signaling.

Another clinically relevant model of IBD was reproduced by dextran sulfate sodium (DSS) administration and disease progression was determined by disease activity index (DAI), which accounts for pathologic symptoms including bloody and loose stool. Consistent with previous data and compared to Vehicle alone, exposure of mice to DSS/Vehicle in drinking water induced IBD, which progressively increased DAI between days 4 and 6 (Fig. 6A, hatched bars). In comparison, treatment of animals with ABC1183 (50 mg/kg, once daily) dramatically decreased overall disease intensity between days 4 to 6 (Fig. 6A, gray bars). Additionally, colon

length, which shortens following DSS-induced colitis and is indicative of overall damage and scarring, was measured. Compared to vehicle treatment, colons from DSS-treated mice were significantly shortened, while the colon lengths of ABC1183-treated mice were indistinguishable from controls (Fig. 6B). To measure the colonic neutrophil infiltration due to elevated inflammation, which contributes to IBD tissue damage, myeloperoxidase (MPO) activity was quantified from day 6 colons. As indicated in Figure 6C, DSS treatment significantly increased MPO activity, compared to vehicle, while DSS in combination with ABC1183 attenuated neutrophil influx and resultant MPO activity. The findings from DAI score, colon length and MPO activity combine to demonstrate that ABC1183 effectively attenuates pro-inflammatory signaling that drives symptoms of IBD. To further examine the impact of ABC1183 on inflammation signaling, cytokine levels were analyzed from colon samples. DSS-treatment corresponded with increased pro-inflammatory TNFα and IL-6 cytokines and decreased anti-inflammatory IL-10 (Fig. 6D, hatched bars). In contrast, ABC1183 reversed IL-6 and IL-10 expression patterns, but did not influence TNF-α levels (Fig. 6D, gray bars). Overall, these findings promote the hypothesis that the novel GSK3α/β and CDK9 inhibitor, ABC1183, negatively regulates cell growth and pro-inflammatory signaling that is sufficient to abrogate tumor proliferation and IBD progression.

Discussion

Previous studies exploring the impact of GSK3 demonstrate both tumor suppressor and oncogenic capabilities, while dual GSK3/CDK9 inhibitors are often non-selective and target multiple CDKs. Here, we present data demonstrating the selective GSK3 and CDK9 inhibitory function of a novel aromatic DAT, ABC1183. This compound inhibits growth against a broad panel of cancer cell lines with IC_{50} values ranging from 63 nM to 2.8 μM. ABC1183 treatment decreases cell survival through G2/M arrest and modulates GSK3 and CDK9 activity as indicated by changes in GSK3, GS, β-catenin phosphorylation, Pol2 phosphorylation and

MCL1 expression. Additionally, oral administration diminishes tumor growth in multiple animal models, reverses inflammation-driven gastrointestinal disease symptoms, due in part to pro- and anti-inflammatory cytokine modulation, and does not promote any associated gross toxicities. Therefore, ABC1183 is strategically poised to effectively mitigate multiple clinically relevant diseases.

Based on the data, it is hypothesized that ABC1183 inhibits cell proliferation and tumor growth of various cancer types by specifically attenuating GSK3 and CDK9 activity. Both molecules were identified from a human kinome screen for selective inhibition by ABC1183. CDK9 specificity was further queried by analyzing Pol2 and MCL1 expression, which were decreased. Interestingly, ABC1183 altered GSK3 activity based on decreased GSK3α/β and GS phosphorylation and increased β-catenin phosphorylation. These findings are in conflict with canonical GSK3 signaling, whereby inhibition promotes auto-inhibitory pSer21/9 and subsequent decrease of GS phosphorylation. Therefore, ABC1183 treatment causes a mechanistic paradox of signaling output. Treatment with LY2090314, a known GSK3 inhibitor, decreased GSK3 and GS phosphorylation similarly to ABC1183 (Figure 3A, B and C lane 5). Findings herein have been corroborated by other GSK3 inhibitor studies. Treatment of renal cancer cells with GSK3 inhibitor, 9-ING-41, caused G2/M arrest, tumor growth inhibition, and decreased pGS. (Pal et al. 2014). Similarly SB216763 inhibitor decreased GSK3β pSer9 (Hilliard et al. 2011; Koo et al. 2014) and decreased pGS (Benakanakere et al. 2010; Wang et al. 2011). In hepatocellular carcinoma, stemness was conferred through increased GSK3 Ser9 phosphorylation and subsequent stabilization of β-catenin expression (Chua et al. 2015). Therefore, despite the current understanding of GSK3 activity, the disparate findings reported here and elsewhere demonstrate the depth of complexity and cross-talk.

GSK3-mediated phosphorylation of β-catenin signals proteasomal degradation and inhibition of pro-growth target genes (Shang et al. 2017). However, based upon data herein,

ABC1183 treatment increases β-catenin serine phosphorylation, despite inhibiting GSK3 activity. We hypothesize that the reported findings of ABC1183 inhibition is due to the differential priming requirement for substrates. In general, GSK3 substrates require a priming step for engagement within the binding pocket (Beurel et al. 2015). β-catenin phosphorylation within the destruction complex is one example, however, whereby GSK3-mediated phosphorylation is independent of pSer21/9 status (Stamos and Weis 2013). Therefore, although ABC1183 impinges on pSer21/9, it does not negatively affect the ability of GSK3 to signal through a separate pool of β-catenin.

ABC1183 specifically inhibits GSK3 and CDK9 but no other closely related CDK molecules, which is unique since previously described dual inhibitors typically antagonized CDKs broadly, such as Flavopiridol, AT7519 and Roscovitine. Flavopiridol is a pan-CDK inhibitor that targets CDKs 2, 4/6, 7 and 9, and has been in clinical studies since 1994 for numerous tumor types. Although cell proliferation was abrogated via G2/m cell cycle arrest by ABC1183, this result is not specifically attributed to GSK3 and CDK9. AT7519 is a pan CDK inhibitor that similarly caused G2/M arrest and decreased GSK3β ser9 phosphorylation. Multiple phase II clinical trials have been completed but, although treatment is well tolerated, low response rates were observed (Seftel et al. 2017). Therefore, ABC1183 represents a novel molecule for selectively inhibiting CDK9 and GSK3.

ABC1183 treatment of multiple allogenic tumor types significantly reduces growth kinetics, relative to vehicle conditions. Within tumor specimen, GSK3 signaling is inhibited based on reduced GSK3 and GS serine phosphorylation, which is consistent with cellular findings. These data confirm that ABC1183 engages the anticipated targets and sufficiently abrogates tumor progression. In pre-clinical and clinical scenarios, post-translation modifications, rather than GSK3 expression, was most frequently associated with disease state and numerous

studies support the biological relevance of GSK3 signaling in cancer progression. In cell-based models, GSK3β Ser9 levels corresponded with cisplatin resistance in ovarian cancer cells (Cai et al. 2007) and antagonized cell apoptosis (Gao et al. 2014). Novel AKT and AGC kinase family inhibitors decreased pSer21/9 GSK3α/β, which corresponded with decreased cancer cell survival (Yap et al. 2012; Yap et al. 2011). In a retrospective analysis, GSK3 pSer9 was present in 47% of invasive mammary carcinomas and correlated with a worse clinical outcome (Armanious et al. 2010), and also correlated with a poor prognosis in a lung carcinomas (Zheng et al. 2007). A Phase II trial investigating LY treatment for AML patients demonstrated on-target effects based on β-catenin expression, however limited clinical benefit was observed (Rizzieri et al. 2016). Phase I/II trial with the Protein Kinase C inhibitor, enzastaurin, which decreased GSK3β phosphorylation in culture (Graff et al. 2005), was shown to decrease pSer9 in peripheral blood monocytes from patients with high-grade glioma (Kreisl et al. 2010). Therefore, these studies corroborate the biological significance and utility for intratumoral detection of protein phosphorylation states as clinically relevant biomarker options.

Multiple models of inflammation-driven gastrointestinal disease provide evidence that ABC1183 effectively attenuates pro-inflammatory cytokines, TNF-α and IL-6, increases anti-inflammatory cytokine, IL-10, modulates immune cell infiltration and, subsequently, diminishes symptoms of disease. These results underscore the pro-inflammatory role of both GSK3 and CDK9 implicated in many disease types. GSK3 regulates multiple mechanisms promoting inflammation, however, paramount is the transcriptional activity of NF-κB. GSK3 inhibition decreases nuclear accumulation of NF-κB and regulates cytokine production (Cortes-Vieyra et al. 2012), similar to our findings. CDK9 also influences inflammatory immune response by promoting expression of pro-inflammatory cytokine genes (Brasier 2008; Brasier et al. 2011) and the extravasation of leukocytes into sites of inflammation (Berberich et al. 2011). NF-κB is

also a dominant player in this signaling as pNF-κB is required for CDK9 incorporation into P-TEFb (Fang et al. 2014; Nowak et al. 2008). These overlapping mechanisms of inflammation have profound implications as elevated inflammation is also associated with neurological disorders, such as Alzheimer's and Parkinson's disease, gastrointestinal disorders, cancer and others (Kalia and Lang 2015; Morales et al. 2014). Furthermore, given that the described tumor studies herein utilized immune-competent animals, the anti-tumor function of ABC1183 could be associated with reduced NF-κB signaling and suppressed pro-inflammatory production. Future studies will characterize tumor-associated inflammation and the ability of ABC1183 to resolve symptoms associated with inflammation in neurologic diseases.

ABC1183 is a novel small molecule dual inhibitor of GSK3 and CDK9 that is effective as a single agent to inhibit clinically relevant models of disease. Mechanistic studies highlight the anti-proliferative capability of ABC1183 and underscore the complex GSK3 and CDK9 signaling networks. ABC1183 inhibits pre-clinical models of tumor growth as an orally available single agent with on-target action. Pharmacodynamic biomarkers are advantageous to monitor treatment efficacy from tumor biopsies. We have also demonstrated the potent anti-inflammatory effect of dual GSK3 and CDK9 abrogation and the ability to antagonize cytokine-induced inflammatory disease. Overall, ABC1183 is positioned to progress into further development for clinical investigation.

Acknowledgements

Authorship contributions

Participated in research design: Schrecengost, Maines, CD Smith

Conducted experiments: Schrecengost, Green, Keller, RA Smith, Maines

Contributed new reagents or analytic tools: Zhuang

Performed data analysis: Schrecengost, Keller, RA Smith, Maines

Wrote or contributed to the writing of the manuscript: Schrecengost, Green, Smith

References

Armanious H, Deschenes J, Gelebart P, Ghosh S, Mackey J, Lai R (2010) Clinical and biological significance of GSK-3beta inactivation in breast cancer-an immunohistochemical study. Human pathology 41: 1657-1663

Benakanakere MR, Zhao J, Galicia JC, Martin M, Kinane DF (2010) Sphingosine kinase-1 is required for toll mediated beta-defensin 2 induction in human oral keratinocytes. PloS one 5: e11512

Berberich N, Uhl B, Joore J, Schmerwitz UK, Mayer BA, Reichel CA, Krombach F, Zahler S, Vollmar AM, Furst R (2011) Roscovitine blocks leukocyte extravasation by inhibition of cyclin-dependent kinases 5 and 9. British journal of pharmacology 163: 1086-1098

Beurel E, Grieco SF, Jope RS (2015) Glycogen synthase kinase-3 (GSK3): regulation, actions, and diseases. Pharmacology & therapeutics 148: 114-131

Beurel E, Michalek SM, Jope RS (2010) Innate and adaptive immune responses regulated by glycogen synthase kinase-3 (GSK3). Trends in immunology 31: 24-31

Brasier AR (2008) Expanding role of cyclin dependent kinases in cytokine inducible gene expression. Cell cycle 7: 2661-2666

Brasier AR, Tian B, Jamaluddin M, Kalita MK, Garofalo RP, Lu M (2011) RelA Ser276 phosphorylation-coupled Lys310 acetylation controls transcriptional elongation of inflammatory cytokines in respiratory syncytial virus infection. Journal of virology 85: 11752-11769

Cai G, Wang J, Xin X, Ke Z, Luo J (2007) Phosphorylation of glycogen synthase kinase-3 beta at serine 9 confers cisplatin resistance in ovarian cancer cells. International journal of oncology 31: 657-662

Chua HH, Tsuei DJ, Lee PH, Jeng YM, Lu J, Wu JF, Su DS, Chen YH, Chien CS, Kao PC, Lee CN, Hu RH, Ni YH, Chang MH (2015) RBMY, a novel inhibitor of glycogen synthase kinase 3beta, increases tumor stemness and predicts poor prognosis of hepatocellular carcinoma. Hepatology 62: 1480-1496

Cortes-Vieyra R, Bravo-Patino A, Valdez-Alarcon JJ, Juarez MC, Finlay BB, Baizabal-Aguirre VM (2012) Role of glycogen synthase kinase-3 beta in the inflammatory response caused by bacterial pathogens. Journal of inflammation 9: 23

Cross DA, Alessi DR, Cohen P, Andjelkovich M, Hemmings BA (1995) Inhibition of glycogen synthase kinase-3 by insulin mediated by protein kinase B. Nature 378: 785-789

Duffy DJ, Krstic A, Schwarzl T, Higgins DG, Kolch W (2014) GSK3 inhibitors regulate MYCN mRNA levels and reduce neuroblastoma cell viability through multiple mechanisms, including p53 and Wnt signaling. Molecular cancer therapeutics 13: 454-467

Eldar-Finkelman H, Martinez A (2011) GSK-3 Inhibitors: Preclinical and Clinical Focus on CNS. Front Mol Neurosci 4: 32

Fang L, Choudhary S, Zhao Y, Edeh CB, Yang C, Boldogh I, Brasier AR (2014) ATM regulates NF-kappaB-dependent immediate-early genes via RelA Ser 276 phosphorylation coupled to CDK9 promoter recruitment. Nucleic acids research 42: 8416-8432

Fang X, Yu SX, Lu Y, Bast RC, Jr., Woodgett JR, Mills GB (2000) Phosphorylation and inactivation of glycogen synthase kinase 3 by protein kinase A. Proceedings of the National Academy of Sciences of the United States of America 97: 11960-11965

Fitzpatrick LR, Wang J, Le T (2000) In vitro and in vivo effects of gliotoxin, a fungal metabolite: efficacy against dextran sodium sulfate-induced colitis in rats. Digestive diseases and sciences 45: 2327-2336

Gao X, He Y, Gao LM, Feng J, Xie Y, Liu X, Liu L (2014) Ser9-phosphorylated GSK3beta induced by 14-3-3zeta actively antagonizes cell apoptosis in a NF-kappaB dependent manner. Biochemistry and cell biology = Biochimie et biologie cellulaire 92: 349-356

Graff JR, McNulty AM, Hanna KR, Konicek BW, Lynch RL, Bailey SN, Banks C, Capen A, Goode R, Lewis JE, Sams L, Huss KL, Campbell RM, Iversen PW, Neubauer BL, Brown TJ,

Musib L, Geeganage S, Thornton D (2005) The protein kinase Cbeta-selective inhibitor, Enzastaurin (LY317615.HCl), suppresses signaling through the AKT pathway, induces apoptosis, and suppresses growth of human colon cancer and glioblastoma xenografts. Cancer research 65: 7462-7469
Gregory GP, Hogg SJ, Kats LM, Vidacs E, Baker AJ, Gilan O, Lefebure M, Martin BP, Dawson MA, Johnstone RW, Shortt J (2015) CDK9 inhibition by dinaciclib potently suppresses Mcl-1 to induce durable apoptotic responses in aggressive MYC-driven B-cell lymphoma in vivo. Leukemia 29: 1437-1441
Ha NC, Tonozuka T, Stamos JL, Choi HJ, Weis WI (2004) Mechanism of phosphorylation-dependent binding of APC to beta-catenin and its role in beta-catenin degradation. Molecular cell 15: 511-521
Haque A, Koide N, Iftakhar EKI, Noman AS, Odkhuu E, Badamtseren B, Naiki Y, Komatsu T, Yoshida T, Yokochi T (2011) Flavopiridol inhibits lipopolysaccharide-induced TNF-alpha production through inactivation of nuclear factor-kappaB and mitogen-activated protein kinases in the MyD88-dependent pathway. Microbiology and immunology 55: 160-167
Hilliard TS, Gaisina IN, Muehlbauer AG, Gaisin AM, Gallier F, Burdette JE (2011) Glycogen synthase kinase 3beta inhibitors induce apoptosis in ovarian cancer cells and inhibit in-vivo tumor growth. Anti-cancer drugs 22: 978-985
Hofmann C, Dunger N, Scholmerich J, Falk W, Obermeier F (2010) Glycogen synthase kinase 3-beta: a master regulator of toll-like receptor-mediated chronic intestinal inflammation. Inflammatory bowel diseases 16: 1850-1858
Jafari R, Almqvist H, Axelsson H, Ignatushchenko M, Lundback T, Nordlund P, Martinez Molina D (2014) The cellular thermal shift assay for evaluating drug target interactions in cells. Nature protocols 9: 2100-2122
Kalia LV, Lang AE (2015) Parkinson's disease. Lancet 386: 896-912
Keum YS, Kim HG, Bode AM, Surh YJ, Dong Z (2013) UVB-induced COX-2 expression requires histone H3 phosphorylation at Ser10 and Ser28. Oncogene 32: 444-452
Koo J, Yue P, Gal AA, Khuri FR, Sun SY (2014) Maintaining glycogen synthase kinase-3 activity is critical for mTOR kinase inhibitors to inhibit cancer cell growth. Cancer research 74: 2555-2568
Kreisl TN, Kotliarova S, Butman JA, Albert PS, Kim L, Musib L, Thornton D, Fine HA (2010) A phase I/II trial of enzastaurin in patients with recurrent high-grade gliomas. Neuro-oncology 12: 181-189
Krystof V, Baumli S, Furst R (2012) Perspective of cyclin-dependent kinase 9 (CDK9) as a drug target. Current pharmaceutical design 18: 2883-2890
Lam LT, Pickeral OK, Peng AC, Rosenwald A, Hurt EM, Giltnane JM, Averett LM, Zhao H, Davis RE, Sathyamoorthy M, Wahl LM, Harris ED, Mikovits JA, Monks AP, Hollingshead MG, Sausville EA, Staudt LM (2001) Genomic-scale measurement of mRNA turnover and the mechanisms of action of the anti-cancer drug flavopiridol. Genome biology 2: RESEARCH0041
Maines LW, Fitzpatrick LR, French KJ, Zhuang Y, Xia Z, Keller SN, Upson JJ, Smith CD (2008) Suppression of ulcerative colitis in mice by orally available inhibitors of sphingosine kinase. Digestive diseases and sciences 53: 997-1012
Maines LW, Fitzpatrick LR, Green CL, Zhuang Y, Smith CD (2010) Efficacy of a novel sphingosine kinase inhibitor in experimental Crohn's disease. Inflammopharmacology 18: 73-85
Martinez Molina D, Jafari R, Ignatushchenko M, Seki T, Larsson EA, Dan C, Sreekumar L, Cao Y, Nordlund P (2013) Monitoring drug target engagement in cells and tissues using the cellular thermal shift assay. Science 341: 84-87
Morales F, Giordano A (2016) Overview of CDK9 as a target in cancer research. Cell cycle 15: 519-527

Morales I, Guzman-Martinez L, Cerda-Troncoso C, Farias GA, Maccioni RB (2014) Neuroinflammation in the pathogenesis of Alzheimer's disease. A rational framework for the search of novel therapeutic approaches. Frontiers in cellular neuroscience 8: 112
Nowak DE, Tian B, Jamaluddin M, Boldogh I, Vergara LA, Choudhary S, Brasier AR (2008) RelA Ser276 phosphorylation is required for activation of a subset of NF-kappaB-dependent genes by recruiting cyclin-dependent kinase 9/cyclin T1 complexes. Molecular and cellular biology 28: 3623-3638
Pal K, Cao Y, Gaisina IN, Bhattacharya S, Dutta SK, Wang E, Gunosewoyo H, Kozikowski AP, Billadeau DD, Mukhopadhyay D (2014) Inhibition of GSK-3 induces differentiation and impaired glucose metabolism in renal cancer. Molecular cancer therapeutics 13: 285-296
Rayasam GV, Tulasi VK, Sodhi R, Davis JA, Ray A (2009) Glycogen synthase kinase 3: more than a namesake. British journal of pharmacology 156: 885-898
Rizzieri DA, Cooley S, Odenike O, Moonan L, Chow KH, Jackson K, Wang X, Brail L, Borthakur G (2016) An open-label phase 2 study of glycogen synthase kinase-3 inhibitor LY2090314 in patients with acute leukemia. Leukemia & lymphoma 57: 1800-1806
Schild C, Wirth M, Reichert M, Schmid RM, Saur D, Schneider G (2009) PI3K signaling maintains c-myc expression to regulate transcription of E2F1 in pancreatic cancer cells. Molecular carcinogenesis 48: 1149-1158
Schrecengost RS, Keller SN, Schiewer MJ, Knudsen KE, Smith CD (2015) Downregulation of Critical Oncogenes by the Selective SK2 Inhibitor ABC294640 Hinders Prostate Cancer Progression. Molecular cancer research : MCR 13: 1591-1601
Seftel MD, Kuruvilla J, Kouroukis T, Banerji V, Fraser G, Crump M, Kumar R, Chalchal HI, Salim M, Laister RC, Crocker S, Gibson SB, Toguchi M, Lyons JF, Xu H, Powers J, Sederias J, Seymour L, Hay AE (2017) The CDK inhibitor AT7519M in patients with relapsed or refractory chronic lymphocytic leukemia (CLL) and mantle cell lymphoma. A Phase II study of the Canadian Cancer Trials Group. Leukemia & lymphoma 58: 1358-1365
Shang S, Hua F, Hu ZW (2017) The regulation of beta-catenin activity and function in cancer: therapeutic opportunities. Oncotarget 8: 33972-33989
Sonawane YA, Taylor MA, Napoleon JV, Rana S, Contreras JI, Natarajan A (2016) Cyclin Dependent Kinase 9 Inhibitors for Cancer Therapy. Journal of medicinal chemistry 59: 8667-8684
Stamos JL, Weis WI (2013) The beta-catenin destruction complex. Cold Spring Harbor perspectives in biology 5: a007898
Takada Y, Aggarwal BB (2004) Flavopiridol inhibits NF-kappaB activation induced by various carcinogens and inflammatory agents through inhibition of IkappaBalpha kinase and p65 phosphorylation: abrogation of cyclin D1, cyclooxygenase-2, and matrix metalloprotease-9. The Journal of biological chemistry 279: 4750-4759
Thomas NE, Thamkachy R, Sivakumar KC, Sreedevi KJ, Louis XL, Thomas SA, Kumar R, Rajasekharan KN, Cassimeris L, Sengupta S (2014) Reversible action of diaminothiazoles in cancer cells is implicated by the induction of a fast conformational change of tubulin and suppression of microtubule dynamics. Molecular cancer therapeutics 13: 179-189
Vasudevan S, Thomas SA, Sivakumar KC, Komalam RJ, Sreerekha KV, Rajasekharan KN, Sengupta S (2015) Diaminothiazoles evade multidrug resistance in cancer cells and xenograft tumour models and develop transient specific resistance: understanding the basis of broad-spectrum versus specific resistance. Carcinogenesis 36: 883-893
Vincent EE, Elder DJ, O'Flaherty L, Pardo OE, Dzien P, Phillips L, Morgan C, Pawade J, May MT, Sohail M, Hetzel MR, Seckl MJ, Tavare JM (2014) Glycogen synthase kinase 3 protein kinase activity is frequently elevated in human non-small cell lung carcinoma and supports tumour cell proliferation. PloS one 9: e114725
Walz A, Ugolkov A, Chandra S, Kozikowski A, Carneiro BA, O'Halloran TV, Giles FJ, Billadeau DD, Mazar AP (2017) Molecular Pathways: Revisiting Glycogen Synthase Kinase-3beta as a

Target for the Treatment of Cancer. Clinical cancer research : an official journal of the American Association for Cancer Research 23: 1891-1897
Wang H, Brown J, Garcia CA, Tang Y, Benakanakere MR, Greenway T, Alard P, Kinane DF, Martin M (2011) The role of glycogen synthase kinase 3 in regulating IFN-beta-mediated IL-10 production. Journal of immunology 186: 675-684
Yap TA, Walton MI, Grimshaw KM, Te Poele RH, Eve PD, Valenti MR, de Haven Brandon AK, Martins V, Zetterlund A, Heaton SP, Heinzmann K, Jones PS, Feltell RE, Reule M, Woodhead SJ, Davies TG, Lyons JF, Raynaud FI, Eccles SA, Workman P, Thompson NT, Garrett MD (2012) AT13148 is a novel, oral multi-AGC kinase inhibitor with potent pharmacodynamic and antitumor activity. Clinical cancer research : an official journal of the American Association for Cancer Research 18: 3912-3923
Yap TA, Walton MI, Hunter LJ, Valenti M, de Haven Brandon A, Eve PD, Ruddle R, Heaton SP, Henley A, Pickard L, Vijayaraghavan G, Caldwell JJ, Thompson NT, Aherne W, Raynaud FI, Eccles SA, Workman P, Collins I, Garrett MD (2011) Preclinical pharmacology, antitumor activity, and development of pharmacodynamic markers for the novel, potent AKT inhibitor CCT128930. Molecular cancer therapeutics 10: 360-371
Zheng H, Saito H, Masuda S, Yang X, Takano Y (2007) Phosphorylated GSK3beta-ser9 and EGFR are good prognostic factors for lung carcinomas. Anticancer research 27: 3561-3569

Footnotes:

a) This work was supported by a grant from the Commonwealth of Pennsylvania, Department of Health

b) Portions of these data were presented at AACR-NCI-EORTC International Conference on Molecular Targets and Cancer Therapeutics: Discovery, Biology, and Clinical Applications, 2016..

c) Reprint requests should be directed to Charles D Smith 1214 Research Blvd, Suite 2014 Hummelstown PA 17036, cdsmith@apogee-biotech.com

Figure Legend

Figure 1. ABC1183 selectively inhibits GSK3 α/β and CDK9. (A) Structure of ABC1183. (B) *top, in vitro* kinase screen with 10uM ABC1183 and graphical representation of inhibition. *Bottom,* 4 kinases with inhibition >60%. (C) Dose response assay calculating IC_{50} values of GSK3α, GSK3β and CDK9.

Figure 2. ABC1183 exhibits cytotoxicity against a panel of murine and human cancer cells. (A) The indicated cell lines were seeded into 96 well plates at determined sub-confluent concentrations and 24 hours later were treated with a dose response of ABC1183 for 72 hours. Cell survival was quantified by sulforhodamine B assay. IC_{50} value for each cell line shown. (B) Pan02 cells were treated with DMSO or 3uM ABC1183 for 24 hours and cell cycle was analyzed by propidium iodide staining. Representative histogram plots are shown.

Figure 3. Multiple tumorigenic signaling pathways are inhibited by ABC1183. (A) LNCaP, (B) Pan02, (C) FaDu cells were treated with 3 μM ABC1183 for 2 to 24 hours or 20nM LY2090314 , as indicated. Cell lysates were immunoblotted with MCL1, pSer21/9 GSK3α/β, GSK3β, pSer641 GS, GS, pSer33/37 Thr41 β-catenin, β-catenin and GAPDH.

Figure 4. Inhibition of tumor growth by ABC1183. C57BL/6 mice were injected subcutaneously with (A) B16 melanoma cells suspended in PBS or (B) PAN02 pancreatic cancer cells suspended in PBS/growth matrix or (C) TRAMP-C2 murine prostate cancer cells suspended in PBS/growth matrix. After tumor volume of at least 100 mm^3, animals were treated 5 times per week by oral gavage of either 100 μl Vehicle (open squares), 5 mg/kg ABC1183 (A and B) or 2 mg/kg ABC1183 (C) (gray squares). Tumor volume measurement was performed for timecourse as indicated. n=5 per group in A and C, n=10 per group for B. * $p<0.05$ ** $p<0.01$. (D) Pan02-bearing mice were treated with 5 mg/kg or 25 mg/kg for 2 or 12 hours. Tumors were excised, snap frozen, processed and tumor lysates were immunoblotted with pSer21/9 GSK3α/β, GSK3β, pSer641 GS, and GS.

Figure 5. ABC1183 is safe for oral administration and reduces severity of TNBS-colitis model, at least in part, through inflammatory cytokines. (A). Seven-day toxicity of ABC1183. The indicated dose of ABC1183 was administered by oral gavage daily for 7 days, and the mice were then sacrificed for hematology, blood chemistry and organ weight analyses. Values are mean ± SEM, n =3 or 4 mice/group. (B) C57BL/6 mice were treated with rectal 50% ethanol and oral vehicle (black bars); rectal TNBS and oral vehicle (cross hatched bars) rectal TNBS or oral ABC1183 (gray bars 50 mg/kg). Animals were sacrificed on day 10 and macroscopic inflammation within the distal 3cm of each colon was scored. (C) Mice were treated as in *A* and TNF-α and IL-6 cytokines levels were determined from colon samples. * $p<0.05$ ** $p<0.01$.

Figure 6. Effect of oral ABC1183 on disease parameters in the mouse DSS-induced ulcerative colitis. C57BL/6 mice were treated with oral vehicle (black bars), 2% DSS positive control (horizontal hatched bars) or 2% DSS with oral ABC1183 50mg/kg BID (gray bars) and the following parameters were measured: (A) Disease Activity Index (DAI) which monitors disease severity. (B) Colon length on day six of treatment (C) Myeloperoxidase (MPO) activity was measured from the colons of animals on day 6 of treatment. (D) Cytokine values: TNFα, IL-6 and IL-10 cytokine levels were determined from colon samples. * $p<0.05$ ** $p<0.01$.

Figure 1

A

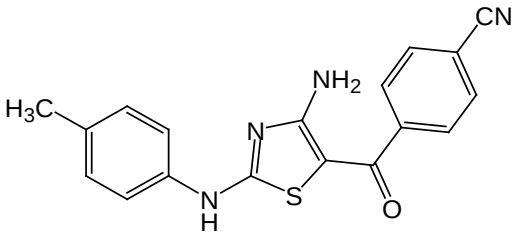

B

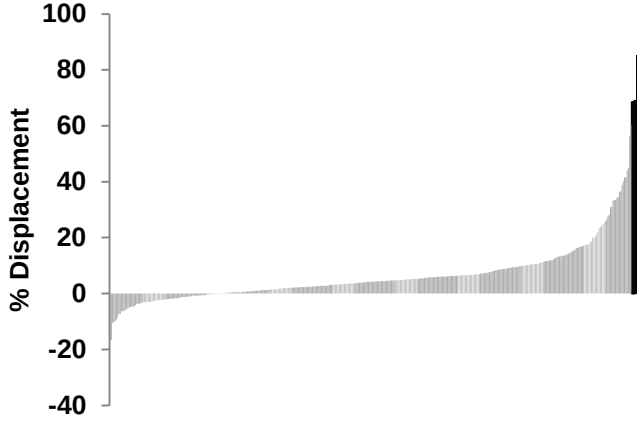

Kinase	ATP Displacement
GSK3α	69%
GSK3β	68%
CDK9 (inactive)	68%
CDK9/cyclin T1	85%

C

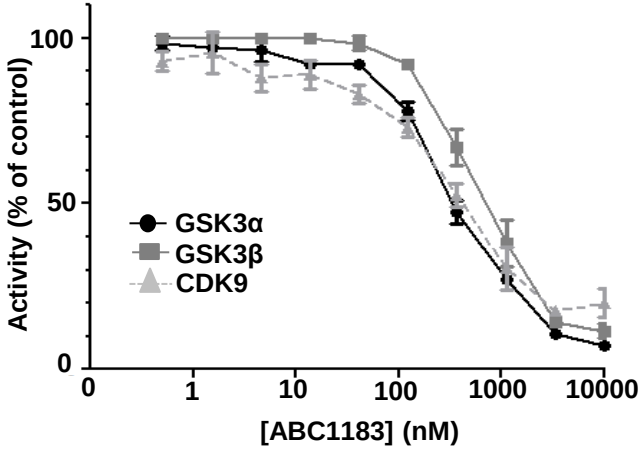

Figure 2

A

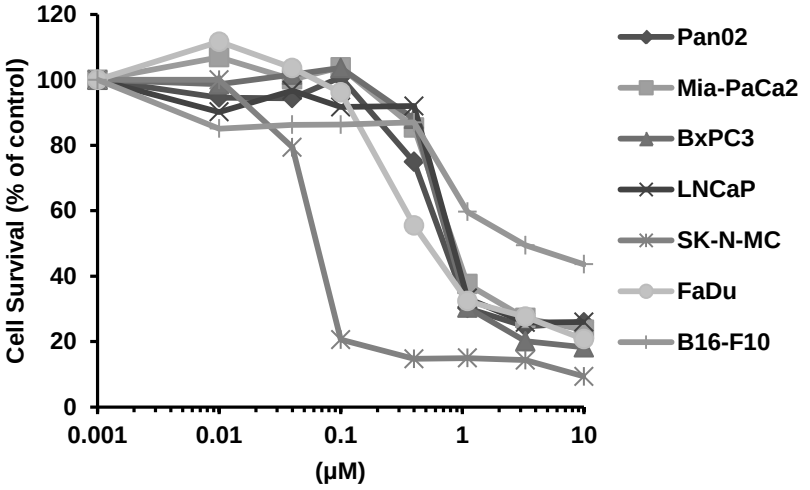

Cell Line	IC_{50} ABC1183
Pan02	678 nM
Mia-Paca2	854 nM
BxPC3	761 nM
LNCaP	790 nM
SK-N-MC	63 nM
FaDu	498 nM
B16-F10	2.8 μM

B

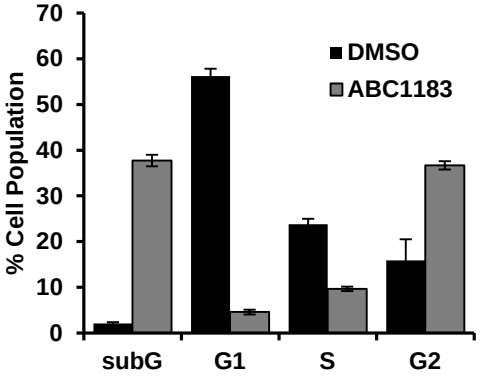

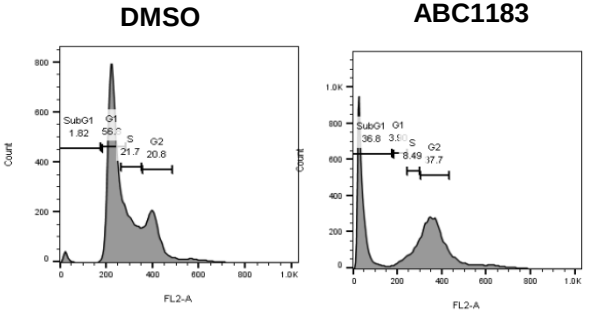

Figure 3

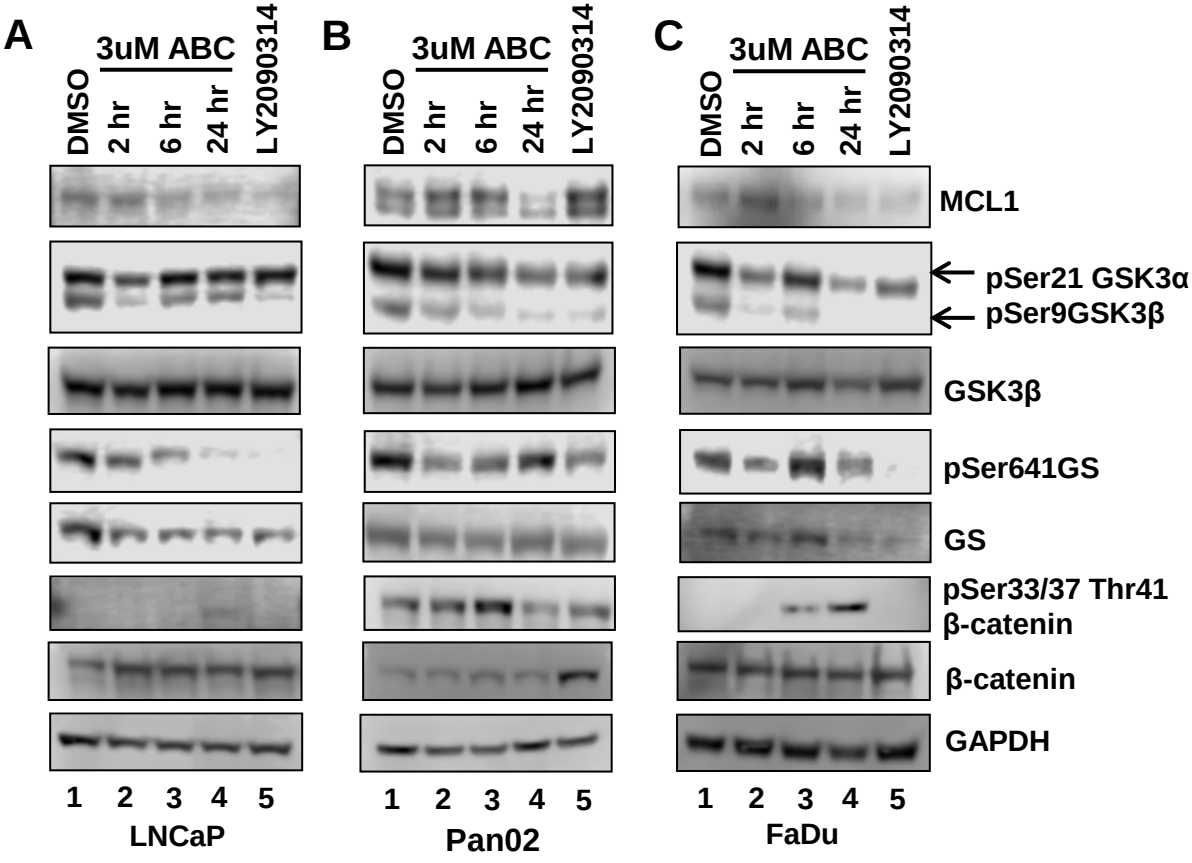
A
3uM ABC
DMSO
2 hr
6 hr
24 hr
LY2090314
B
3uM ABC
DMSO
2 hr
6 hr
24 hr
LY2090314
C
3uM ABC
DMSO
2 hr
6 hr
24 hr
LY2090314
MCL1
pSer21 GSK3α
pSer9GSK3β
GSK3β
pSer641GS
GS
pSer33/37 Thr41
β-catenin
β-catenin
GAPDH
1 2 3 4 5
LNCaP
1 2 3 4 5
Pan02
1 2 3 4 5
FaDu

Figure 4

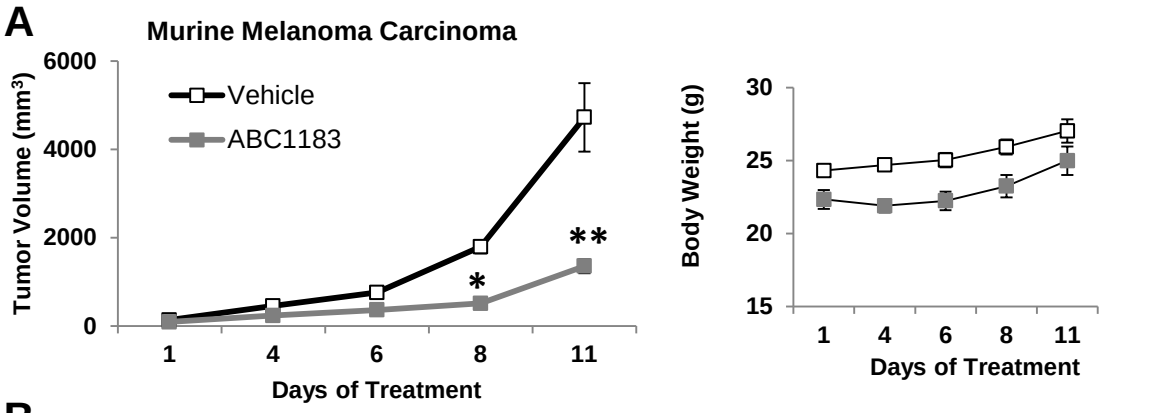
A
Murine Melanoma Carcinoma
Tumor Volume (mm³)
6000
4000
2000
0
Vehicle
ABC1183
*
**
1
4
6
8
11
Days of Treatment
Body Weight (g)
30
25
20
15
1
4
6
8
11
Days of Treatment

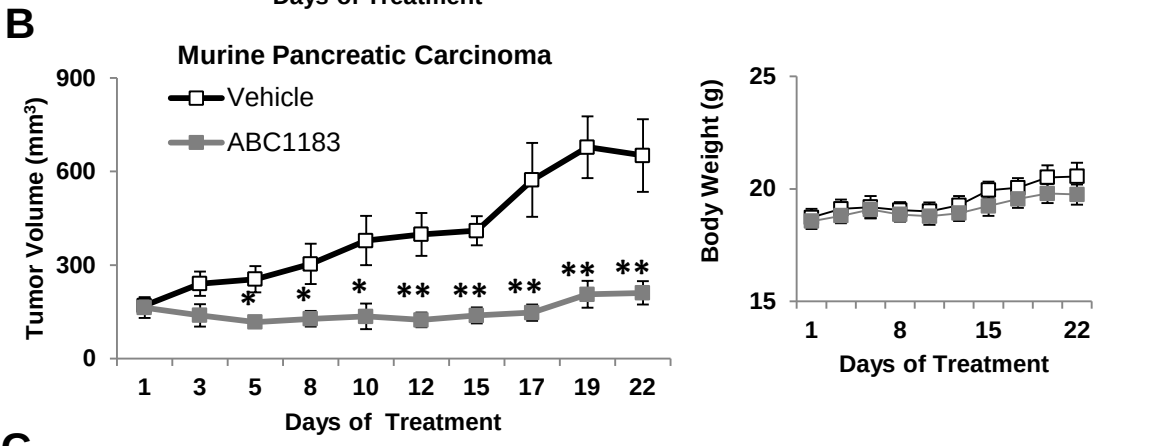
B
Murine Pancreatic Carcinoma
Tumor Volume (mm³)
900
600
300
0
Vehicle
ABC1183
*
**
1
3
5
8
10
12
15
17
19
22
Days of Treatment
Body Weight (g)
25
20
15
1
8
15
22
Days of Treatment

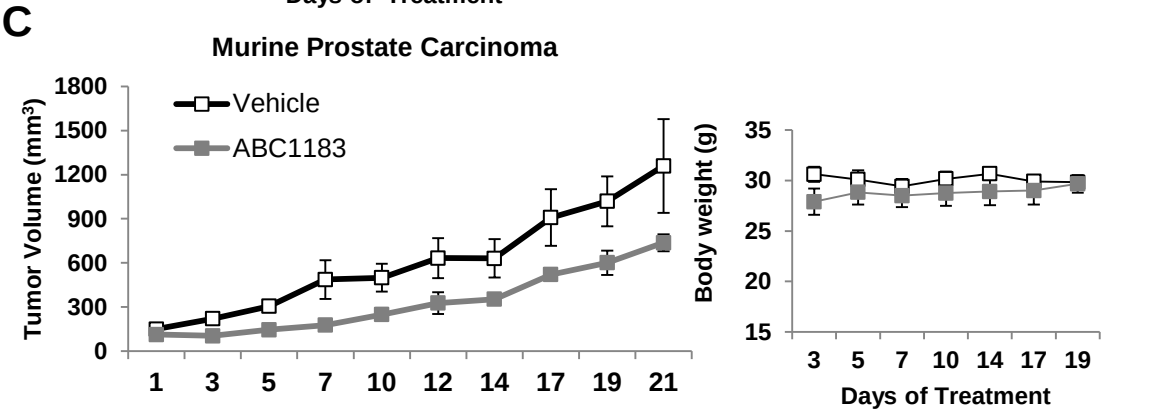
C
Murine Prostate Carcinoma
Tumor Volume (mm³)
1800
1500
1200
900
600
300
0
Vehicle
ABC1183
1
3
5
7
10
12
14
17
19
21
Body weight (g)
35
30
25
20
15
3
5
7
10
14
17
19
Days of Treatment

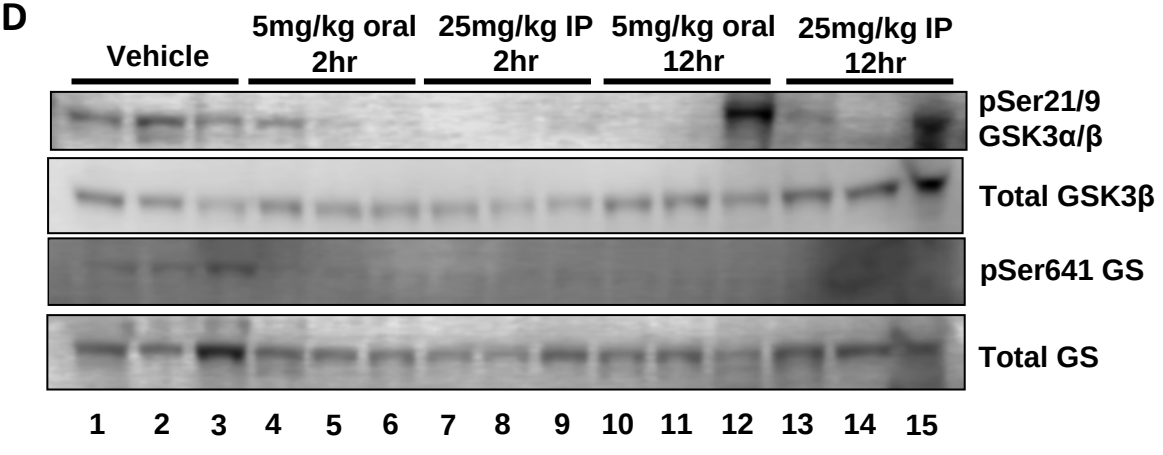
D
Vehicle
5mg/kg oral 2hr
25mg/kg IP 2hr
5mg/kg oral 12hr
25mg/kg IP 12hr
pSer21/9 GSK3α/β
Total GSK3β
pSer641 GS
Total GS
1
2
3
4
5
6
7
8
9
10
11
12
13
14
15

A

Parameter	Vehicle	100 mg/kg	200 mg/kg
Weight loss (%)	0.29±0.17	1.64±0.32	1.16±0.3
Heart weight (g)	0.165±0.004	0.148±0.009	0.1537±0.005
Liver weight (g)	1.383±0.137	1.464±0.008	1.56±0.046
Kidney weight (g)	0.354±0.018	0.346±0.012	0.378±0.009
Red Blood cells ($x10^3mm^3$)	9.26±0.8	9.34±0.11	8.55±0.42
White blood cells ($x10^3mm^3$)	7.45±1.01	6.75±0.75	5.85±0.29
Platelets ($x10^3mm^3$)	1066±93	1401±192	987±118
ALT (IU/L)	14.75±1.89	17.33±3.18	37.0±20.6
Creatinine (mg/dl)	0.20±0.04	0.20±0	0.13±0.03
Glucose (mg/dl)	180±17.2	199.3±10.2	190.3±20.2

B

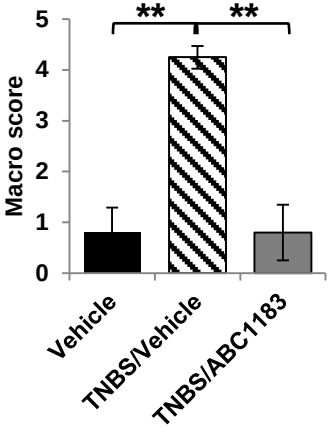

C

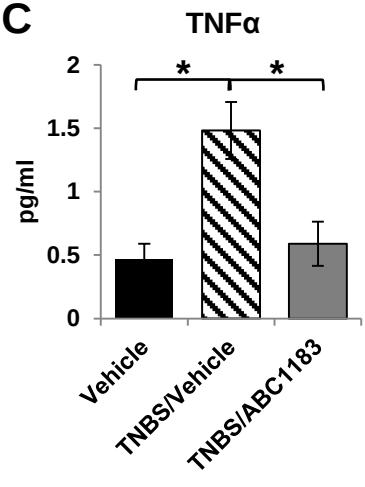

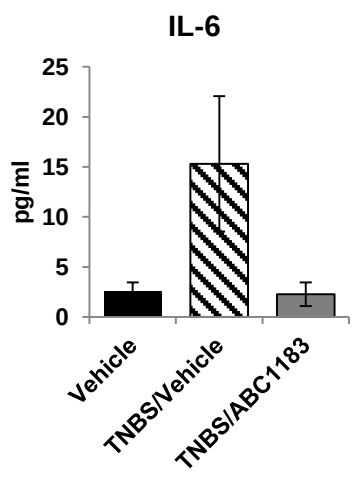

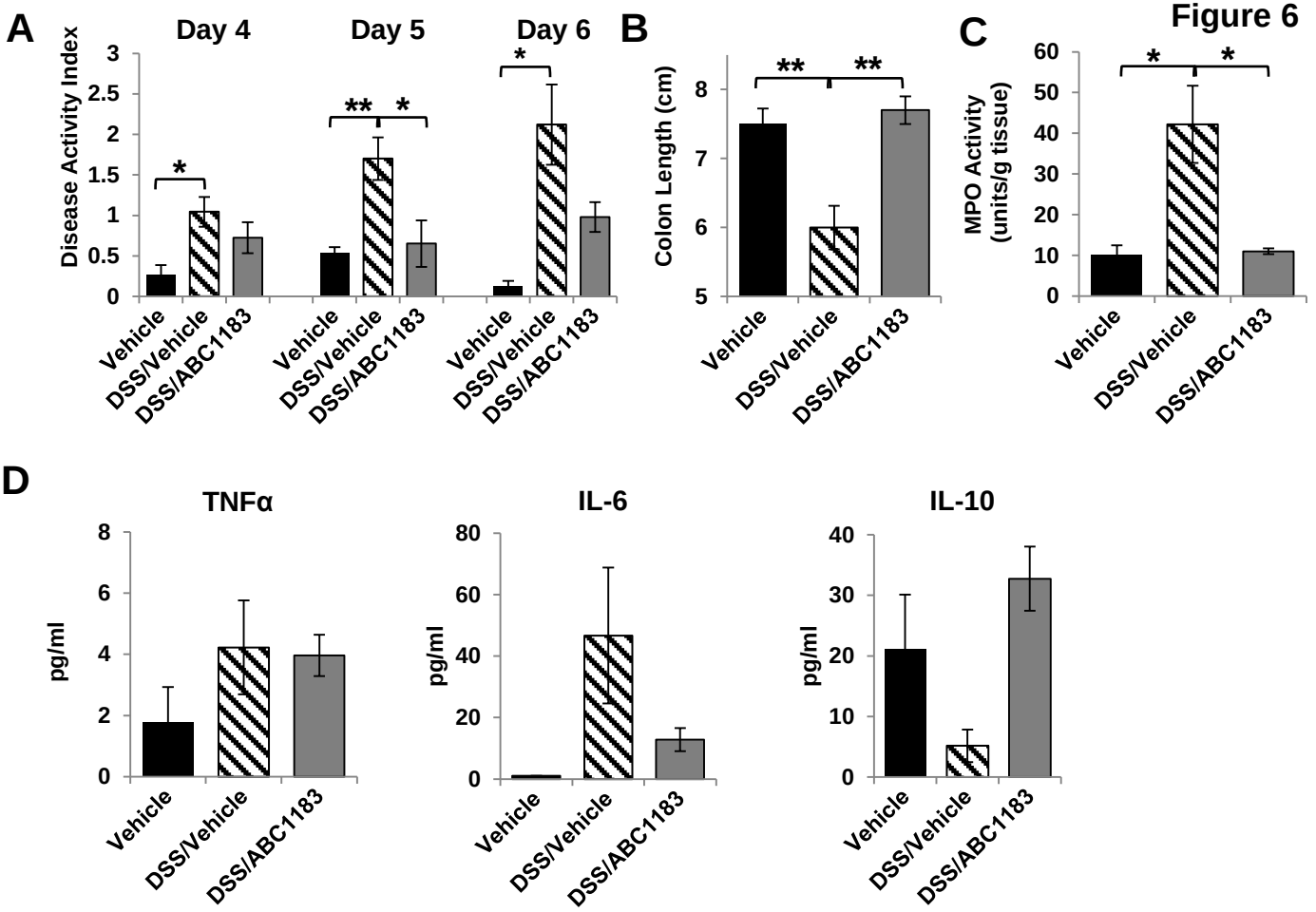
A
Day 4
Day 5
Day 6
Disease Activity Index
3
2.5
2
1.5
1
0.5
0
*
**
*
*
Vehicle
DSS/Vehicle
DSS/ABC1183
B
Colon Length (cm)
8
7
6
5
**
**
Vehicle
DSS/Vehicle
DSS/ABC1183
C
MPO Activity (units/g tissue)
60
50
40
30
20
10
0
*
*
Vehicle
DSS/Vehicle
DSS/ABC1183
D
TNFα
pg/ml
8
6
4
2
0
Vehicle
DSS/Vehicle
DSS/ABC1183
IL-6
pg/ml
80
60
40
20
0
Vehicle
DSS/Vehicle
DSS/ABC1183
IL-10
pg/ml
40
30
20
10
0
Vehicle
DSS/Vehicle
DSS/ABC1183